

82-1551

352
8-18-75

LA-5942-MS

Informal Report

79d

UC 34 and UC-79d

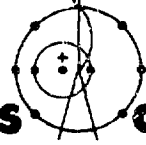
Reporting Date: April 1975

Issued: June 1975

Numerical Calculation of Two-Phase Flows

by

John R. Travis
Francis H. Harlow
Anthony A. Amsden



los alamos
scientific laboratory

of the University of California

LOS ALAMOS, NEW MEXICO 87544

An Affirmative Action/Equal Opportunity Employer

UNITED STATES
ENERGY RESEARCH AND DEVELOPMENT ADMINISTRATION
CONTRACT W 7405-ENG 56

MASTER

DISTRIBUTION OF THIS DOCUMENT UNLIMITED

bar

**In the interest of prompt distribution, this report was not edited by
the Technical Information staff.**

**This work supported by the Reactor Safety Research Division,
US Energy Research and Development Administration.**

**Printed in the United States of America. Available from
National Technical Information Service
U S Department of Commerce
5285 Port Royal Road
Springfield, VA 22151
Price: Printed Copy \$4.00 Microfiche \$2.25**

**This report was prepared as an account of work sponsored
by the United States Government. Neither the United States
nor the United States Energy Research and Development Ad-
ministration, nor any of their employees, nor any of their con-
tractors, subcontractors, or their employees, make any
warranty, express or implied, or assume any legal liability or
responsibility for the accuracy, completeness, or usefulness of
any information, apparatus, product, or process disclosed, or
represents that its use would not infringe privately owned
rights.**

NOTICE

This report was prepared as an account of work sponsored by the United States Government. Neither the United States nor the United States Energy Research and Development Administration, nor any of their employees, nor any of their contractors, subcontractors, or their employees, makes any warranty, express or implied, or assumes any legal liability or responsibility for the accuracy, completeness, or usefulness of any information, apparatus, product or process disclosed, or represents that its use would not infringe privately owned rights.

NUMERICAL CALCULATION OF TWO-PHASE FLOWS

by

John R. Travis
Francis H. Harlow
Anthony A. Amsden

ABSTRACT

The theoretical study of time-varying two-phase flow problems in several space dimensions introduces such a complicated set of coupled nonlinear partial differential equations that numerical solution procedures for high-speed computers are required in almost all but the simplest examples. Efficient attainment of realistic solutions for practical problems requires a finite-difference formulation that is simultaneously implicit in the treatment of mass convection, equations of state, and the momentum coupling between phases. We describe such a method, discuss the equations on which it is based, and illustrate its properties by means of examples. In particular, we emphasize the capability for calculating physical instabilities and other time-varying dynamics, at the same time avoiding numerical instability. The computer code is applicable to problems in reactor safety analysis, the dynamics of fluidized dust beds, raindrops or aerosol transport, and a variety of similar circumstances, including the effects of phase transitions and the release of latent heat or chemical energy.

I. INTRODUCTION

Some important circumstances of fluid flow involve the interpenetration of several different materials. Examples are the passage of raindrops through air, of bubbles or sediments through water, and of gas through a fluidized dust bed. If the embedded material is a single particle, drop, or bubble, then its dynamics and concurrent reaction back onto the fluid may be amenable to relatively simple analysis through the use of a drag function for momentum exchange, a phase transition function for mass exchange, and a heat transfer function for energy exchange. If there are numerous separate pieces of the embedded material, then the dynamics must also include collective effects, which can complicate the theoretical flow analysis almost to intractability.

The usual procedure for a many-particle analysis is to represent the dynamics of each material by means of field variables. Consider a mixture of air

and water in proportions that can vary from small bubbles in a fluid to small droplets in a gas. In each extreme, the disperse material may be closely tied ("frozen in") to the motion of the surrounding continuous phase, so that there is no relative motion, or drift, between them. For intermediate proportions, the added complications include the retarded drift of the dispersed phase, the induced currents in the continuous phase, condensation and evaporation from or to the water vapor in the air, the release or absorption of latent heat, and the resultant effects of buoyancy. At the same time, collective effects profoundly modify the dynamics from what would occur if the dispersed bubbles or droplets were independent. Collisions and interacting wakes alter the momentum exchange, change the mean size scale of the dispersed material, and distort the droplets or bubbles to large departures from sphericity. The variables necessary to describe

these interacting processes must include two different fields of velocity vectors, a void-fraction or porosity function, two fields of temperature, and two (or possibly one) fields of pressure.

More generally, the effects of a spectrum of size scale for the dispersed phase leads to the requirement for a continuum of field velocities, or alternatively for a distribution function like the Maxwell-Boltzmann distribution for molecular velocities in a gas. It is easy to see that the complexities for the analysis of such a system can grow almost without bound, especially if the dispersed phase consists of a variety of different materials with the potentiality for chemical or nuclear reactions occurring during the dynamics. It is therefore easily realized that numerical solutions with high-speed computer offer the only opportunity for realistic theoretical analysis of any but the most simple multiphase flow problems.

The purpose of this report is to describe a recently developed numerical solution procedure called the Implicit, Multi-Field (IMF) technique,¹ which is applicable to the study of time-varying (initial-value) problems in several space dimensions, in which the continuous phase is a liquid or gas flowing at any Mach number from zero (the incompressible limit) to well above unity (the supersonic limit), and the dispersed phase is formed of microscopically incompressible particles or droplets all with the same size scale. Because the details of the numerical technique and associated computer code have been discussed elsewhere,² this report concentrates on a discussion of the fundamental equations, and on the interpretation and accuracy of the numerical solutions.

In particular, we show an alternative derivation of the momentum equations, which avoids some difficulties encountered by previous authors in formulating the pressure-gradient terms. We also discuss the stability of the equations from both the continuum and numerical (finite-difference) points of view. In this regard, three aspects of the matter are of importance:

1. The high-frequency instabilities of the differential equations, which make the formulation "ill-posed," and cannot, in any case, be resolved by the finite-difference equations,

2. The low-frequency instabilities of the differential equations, which represent important physical processes in the time-varying dynamics, and

3. Instabilities that might be introduced by the numerical solution procedure, whose avoidance by implicitness of the formulation or the introduction of dissipation must not be accomplished at the expense of damping the dynamics of interest.

These topics are discussed from an analytical viewpoint, and illustrated by means of results from some computer calculations.

II. STATISTICAL DERIVATION OF THE FIELD EQUATIONS

The field equations for multiphase flow have been derived by many investigators, usually by means of applying the conservation equations for mass, momentum, and energy to the dynamics in some control volume. Difficulties arise in such derivations from the manner by which cuts are made through the material of one phase in order to integrate over the volume of the other, and by the way in which area and volume integrals over a single phase are transformed to integrals around or over the entire control region. Ingenious techniques have been used to accomplish the averaging implied by these transformations, but controversy persists in the literature as to which procedures are correct. In particular, there is disagreement regarding the formulation of the pressure gradient terms in the momentum equations, and controversy continues concerning the requirement for terms included to ensure that the formulation is well posed.

In this section we show that an alternative type of derivation can be employed, avoiding the ambiguities that arise from control-volume techniques. We employ a Liouville equation for the distribution of scale and velocity, and show that moments of the equation enable a relationship to be found between the field properties and the detailed interactions among phases. In addition to avoiding some of the previous derivation difficulties, the Liouville approach forms a consistent basis for the inclusion of various complicated extensions to the field equations, such as close-packed momentum transfer, the effects of a local spectrum of scales, and fluctuational pressure from the disperse phase.

We outline a special case of the derivation from which the extended and more general forms can be constructed. The central function in the derivation is $N(r, \vec{x}, \vec{u}, t)$, which is defined in such a way that $N dr d\vec{x} d\vec{u}$ is the probable number of solid particles with size (e.g., radius) r in the interval dr , position \vec{x} within the interval $d\vec{x}$, and velocity \vec{u} in the interval $d\vec{u}$, at time t . In addition, $m(r)$ is the mass of a particle with size r [e.g., $m(r) = 4\pi r^3 \rho / 3$, in which ρ is the microscopic density of the particulate (dispersed) phase]. From these functions, the following moments can be formed:

$$N_0 = \iiint N m dr d\vec{u} \quad (1)$$

$$\langle u_i \rangle = \iiint N m u_i dr d\vec{u} \quad (2)$$

and

$$N_0 = \iiint N dr d\vec{u} \quad (3)$$

These functions of position and time describe the mass of particulate material per unit total volume, $\langle u_i \rangle$, the mass-averaged component of velocity in direction x_i , $\langle u_i \rangle$, and the number density of the particles, N_0 . Note that the void fraction is given by $1 - (\rho/\rho_0)$.

The fundamental equation for our derivation expresses the conservation of the total number of particles in any volume of r, \vec{x}, \vec{u} space moving with the particles. Thus we neglect fragmentation, coalescence and other processes that would alter the number of particles, the effects of which could be added as a source term to the particle-number conservation equation,

$$\frac{d}{dt} \iiint N dr d\vec{u} d\vec{x} = 0 \quad (4)$$

It is important to note that the total mass of particles in the arbitrary hyperspace volume is not conserved by our expression.

By means of the usual rules for differentiation of an integral, and the condition that the volume of integration is arbitrary, Eq. (4) can be transformed to the following equivalent Liouville Equation:

$$\frac{\partial N}{\partial t} + \frac{\partial}{\partial x_j} \left(N \frac{dx_j}{dt} \right) + \frac{\partial}{\partial u_j} \left(N \frac{du_j}{dt} \right) + \frac{\partial}{\partial r} \left(N \frac{dr}{dt} \right) = 0, \quad (5)$$

in which the total time derivatives are along the dynamically and kinematically allowable paths of the individual particles. Thus, for Eq. (5),

$$\frac{dx_j}{dt} = u_j \quad (6)$$

$$m \frac{du_j}{dt} = F_j \quad (7)$$

and dr/dt is determined from the rate function for phase transition and the geometrical configuration of the particle. Assuming that the particles are spheres, we can write

$$\frac{dm}{dr} = 4\pi \rho r^2,$$

which will allow the mass transfer rate to be related to the rate of change of radius. Indeed, because of the unique relationship in this case between m and r , the distribution function could as well have been $N(m, \vec{x}, \vec{u}, t)$.

Equation (5) describes the dynamics of the single-particle distribution function, and depends only on expressions for the kinematics and dynamics of a single particle. Nevertheless, there are two ways by which this equation can be considered to represent the multiparticle effects of the dispersed phase. One of these is through the force function, F_j , which represents the time-varying force on a single particle, but can contain in its formulation a representation of the average effects on that particle to be expected from surrounding particles. Although this is only an approximate representation of collective effects, which could be improved by the inclusion of integrals over a two-particle distribution function as a source to Eq. (5), we shall see that the present version is entirely sufficient to illustrate the derivation of a correct expression for the pressure-gradient effects in the field equations for momentum. This is because the second way in which Eq. (5) represents the multiparticle

dynamics of the dispersed phase can be demonstrated by certain selected moments of the equation.

In particular, multiply Eq. (5) by $m(r)$ and $m(r)u_i$ and integrate over the entire range of r and \bar{u} values. The results are

$$\frac{\partial \rho^1}{\partial t} + \frac{\partial}{\partial x_j} (\rho^1 \bar{u}_j) + \iint m \frac{\partial}{\partial r} \left(N \frac{dr}{dt} \right) dr d\bar{u} = 0$$

and

$$\begin{aligned} \frac{\partial \rho^1 u_i}{\partial t} + \frac{\partial}{\partial x_j} \iint m N u_i u_j dr d\bar{u} \\ + \iint m u_i \frac{\partial}{\partial u_j} (N F_j / m) dr d\bar{u} \\ + \iint m u_i \frac{\partial}{\partial r} \left(N \frac{dr}{dt} \right) dr d\bar{u} = 0. \end{aligned}$$

Using integration by parts and reducing the results, we can rearrange these mass and momentum equations to the following

$$\frac{\partial \rho^1}{\partial t} + \frac{\partial}{\partial x_j} (\rho^1 \bar{u}_j) = \iint N \frac{dm}{dt} dr d\bar{u}, \quad (8)$$

and

$$\begin{aligned} \frac{\partial \rho^1 u_i}{\partial t} + \frac{\partial \rho^1 u_i u_j}{\partial x_j} = - \frac{\partial}{\partial x_j} \iint N m u_i u_j dr d\bar{u} \\ + \iint N F_i dr d\bar{u} \\ + \iint N u_i \frac{dm}{dt} dr d\bar{u}, \quad (9) \end{aligned}$$

in which $\delta u_i \equiv u_i - \bar{u}_i$.

Equations (8) and (9) are now in the form of field equations for the dispersed phase, derived without recourse to splits or cuts of a control volume into the domains occupied by each phase. They nevertheless express conservation of mass and momentum for any fixed total control volume in space that one wishes to choose. An integral of Eq. (8) over such a control volume shows that the three terms re-

fer, respectively, to the rate of change of dispersed-phase mass in the volume, the convective flux of that mass through the edges of the volume, and the rate of mass conversion to the dispersed phase by means of phase transitions within the volume.

We have, for example, arrived at an expression for convective flux without the explicit requirement for assuming that the volume per unit total volume of the dispersed phase is equal to the area per unit area open for convection. In similar fashion, the terms in Eq. (9) can be interpreted as the rate of change of total dispersed-phase momentum, the contribution to momentum change from the mean convective flux, the fluctuational contribution analogous to a Reynolds stress in turbulent flow, the effect of single-particle forces on the field momentum, and the conversion rate to dispersed-phase momentum from phase transitions.

Equations (8) and (9) have considerable potentiality for interpretation and extensions, some of which will be reported elsewhere. For our present purpose, we limit the discussion to the special case in which

$$N(r, \bar{u}, t) = (r - \bar{r}) \cdot (\bar{u} - \bar{u}) \cdot \rho(\bar{x}, t) / m(r)$$

in which case, Eq. (8) becomes

$$\frac{\partial \rho^1}{\partial t} + \frac{\partial \rho^1 \bar{u}_j}{\partial x_j} = \frac{dm}{dt} \quad (10)$$

and Eq. (9) becomes

$$\frac{\partial \rho^1 u_i}{\partial t} + \frac{\partial \rho^1 u_i u_j}{\partial x_j} = \frac{1}{m(r)} [F_i(\bar{r}, \bar{u}, t) + \bar{u}_i \frac{dm}{dt}]. \quad (11)$$

Suppose for example, that

$$F_i = m g_i - n_j p da \quad (12)$$

in which g_i is the gravitational acceleration, p is the pressure of the contiguous phase, and n_j is an outward unit normal vector on the particle surface at the element of area, da . If the local fluid velocity, v_i , differs from that of the particle velocity, then the pressure integral can be expanded

as a power series in $(v_i - \bar{u}_i)$, such that

$$F_i = mg_i - \int n_i p_0 da + 6\pi\mu \bar{r} (v_i - \bar{u}_i) + \frac{1}{2}\pi \bar{r}^2 C_D \rho_f (v_i - u_i) |v_i - u_i|, \quad (13)$$

in which p_0 is the pressure in the continuous phase in the absence of relative motion between phases. The Stokes-drag term contains μ , the fluid viscosity, and the form drag term contains ρ_f , the fluid density, and C_D , the drag coefficient. Omitted are contributions such as the virtual mass term, which depends on the relative acceleration between fields, and can be systematically included in this derivation.

If an individual particle is small compared with the scale of pressure variations in the continuous phase, then we can approximate

$$-\int n_i p_0 da = -\int \frac{\partial p_0}{\partial x_i} dV = -m \frac{\partial p_0}{\partial x_i}. \quad (14)$$

Note, however, that if the continuous phase is turbulent, then this approximation may not be valid. In that case $\int n_i p_0 da$ must be split into two contributions, one from the mean-flow pressure and the other representing the statistical effects of the small-scale pressure fluctuations, analogous to those of Brownian motion. In any case, the transformation in Eq. (14) is over a single particle, rather than a set of particles in a control volume, and it is this crucial difference from control volume derivations that allows us to avoid the difficulties previously associated with expressing the pressure-gradient effects in the multiphase-flow momentum equations.

With these considerations, Eq. (11) becomes

$$\frac{\partial \rho' \bar{u}_i}{\partial t} + \frac{\partial \rho' \bar{u}_i \bar{u}_j}{\partial x_j} = -(1-\alpha) \frac{\partial p_0}{\partial x_i} + \rho' g_i + \frac{\rho' \bar{u}_i}{m} \frac{dm}{dt} + \frac{3\rho_f (1-\alpha)}{2\bar{r}^2} (v_i - \bar{u}_i) \left(\frac{3\mu}{\bar{r}} + \frac{\bar{r} C_D}{4} |v_i - \bar{u}_i| \right), \quad (15)$$

which shows the void fraction function correctly outside of the pressure gradient term.

To obtain the momentum equation for the continuous phase, one writes the equation for total momentum and subtracts Eq. (15).

III. DRIFT-FLUX APPROXIMATION

The field equations for the fluid and particles are now written with subscripts f and p, respectively, as follows

$$\frac{\partial \rho'_f}{\partial t} + \frac{\partial \rho'_f u_{fj}}{\partial x_j} = 0, \quad (16)$$

$$\frac{\partial \rho'_p}{\partial t} + \frac{\partial \rho'_p u_{pj}}{\partial x_j} = 0, \quad (17)$$

$$\rho'_f \frac{\partial u_{fi}}{\partial t} + \frac{\partial}{\partial x_j} (\rho'_f u_{fi} u_{fj}) = g_i \rho'_f - \alpha \frac{\partial p}{\partial x_i} + K(u_{pi} - u_{fi}), \quad (18)$$

$$\rho'_p \frac{\partial u_{pi}}{\partial t} + \frac{\partial}{\partial x_j} (\rho'_p u_{pi} u_{pj}) = g_i \rho'_p - (1-\alpha) \frac{\partial p}{\partial x_i} + K(u_{fi} - u_{pi}), \quad (19)$$

in which K is a drag function, phase transitions have been neglected, and overbars plus the subscript on p_0 have been omitted.

We now define

$$\rho_t = \rho'_f + \rho'_p$$

and

$$\rho_t u_{ti} = \rho'_f u_{fi} + \rho'_p u_{pi}$$

in such a way that ρ_t is the total mass per unit volume of both phases, and u_{ti} is the mass average velocity so that $\rho_t u_{ti}$ carries the total momentum of the fluid. Then Eqs. (16) and (17) can be added to give

$$\frac{\partial \rho_t}{\partial t} + \frac{\partial \rho_t u_{tj}}{\partial x_j} = 0, \quad (20)$$

and Eqs. (18) and (19) can be added to yield

$$\frac{\partial}{\partial t} (u_{ti}) + \sum_j (\rho_f' u_{fi} u_{fj} + \rho_p' u_{pi} u_{pj}) = \rho_t g_i - \frac{\partial p}{\partial x_i} \quad (21)$$

With some manipulation, the convective flux term in parentheses can be rewritten

$$\rho_t u_{ti} u_{tj} + \frac{\rho_f' \rho_p'}{\rho_t} (u_{fi} - u_{pi}) (u_{fj} - u_{pj}), \quad (22)$$

showing that the effect of relative velocity between the phases can be isolated in one term, the right-hand term in Expression (22). To express this effect in a different way, the two separate momentum equations are rewritten

$$\frac{\partial u_{fi}}{\partial t} + u_{fj} \frac{\partial u_{fi}}{\partial x_j} = g_i - \frac{1}{\rho_f} \frac{\partial p}{\partial x_i} + \frac{K}{\rho_f} (u_{pi} - u_{fi}),$$

and

$$\frac{\partial u_{pi}}{\partial t} + u_{pj} \frac{\partial u_{pi}}{\partial x_j} = g_i - \frac{1}{\rho_p} \frac{\partial p}{\partial x_i} + \frac{K}{(1-\dots)\rho_p} (u_{fi} - u_{pi}),$$

in which ρ_f' and ρ_p' are the unprimed quantities being the microscopic material densities. We subtract these equations from each other and then apply the assumption of quasi-equilibrium, according to which the entire left side of the result is considered negligible. With some algebraic reduction, the result is

$$u_{pi} - u_{fi} = \frac{(1-\dots)(\rho_p - \rho_f)}{K \rho_t} \frac{\partial p}{\partial x_i} \quad (23)$$

Combining Eq. (23) with Expression (22) and inserting into Eq. (21) results in the drift-flux approximation for the mean momentum equation. Alternatively, Eq. (23) can be used in Eqs. (18) and (19) to eliminate the drag function K , or, after elimination of the density derivatives, the results can be put in the especially simple forms

$$\frac{\partial u_{pi}}{\partial t} + u_{pj} \frac{\partial u_{pi}}{\partial x_j} = g_i - \frac{1}{\rho_t} \frac{\partial p}{\partial x_i} \quad (24)$$

and

$$\frac{\partial u_{fj}}{\partial t} + u_{fj} \frac{\partial u_{fj}}{\partial x_j} = g_j - \frac{1}{\rho_t} \frac{\partial p}{\partial x_j} \quad (25)$$

IV. STABILITY OF THE EQUATIONS

Consider the simplest two-phase flow with relative velocity between the phases, namely a homogeneous configuration in which the density of each field is constant in space and time, and equilibrium is maintained by a balance among uniform pressure gradient, constant gravity, and a constant drag force between the material. As an example, such a flow could be realized in an ideal fluidized dust bed, in which the particles are suspended by the upward motion of a fluid or gas through the field of dust. Suppose that a one-dimensional perturbation were introduced along the line of flow of the continuous phase. The question arises regarding the stability of such a perturbation.

Physical reasoning suggests that the perturbation amplitude would grow. Where the particles are "clumped" or closely packed together, the fluid must flow more rapidly through them than nearby where the particulate density is more sparse. Bernoulli's law indicates that the pressure would be lower in such a region of clumping, just as it is in the throat of a Venturi contraction. As a result, particles would accelerate towards the region of clumping and the perturbation amplitude increase. This is a longitudinal variant of the transverse Helmholtz instability, which is driven by a similar variation in pressure along the streamlines on either side of an irregular interface.

A detailed linear stability analysis confirms the intuitive reasoning, and shows in more detail both the growth and propagation of such longitudinal perturbations. In the absence of viscous dissipation, the equations exhibit an instability growth rate that becomes infinite as the perturbation wave length becomes vanishingly small. As a result, the equations are classed as ill-posed,³ and therefore not applicable to the solution of initial-value problems.

In physical reality, the ill-posed nature is precluded by dissipative processes, which are especially effective in damping the highest frequency components of any perturbation, at the same time

having relatively little effect on the larger scale fluctuations. Figure 1 illustrates such a process through a comparison of instability growth rate as a function of perturbation wavelength for various magnitudes of the viscosity coefficient in momentum diffusion terms added to the equations described above. With no dissipation, the growth rate is bounded, but at the same time not strongly displaced from the inviscid growth rate at larger wavelengths. The implications of all this for the numerical solution of the equations is described in the next section.

V. NUMERICAL SOLUTION OF THE EQUATIONS

Application of the two-phase flow equations to the analysis of a specific problem leads to great mathematical complexity in all but the simplest circumstances. For this reason, it has been necessary to develop numerical solution techniques for high-speed computers. Inevitably, such an approach requires the introduction of approximations, usually through the finite-difference representation of both space and time derivative. For this purpose, the spatial domain of interest is divided into a nest of computational cells. The computer then stores for each cell the average values of the various field variables, so that the configuration is described by a finite number of values rather than the infinite number required for the precise description of a continuum. In addition, the calculation proceeds through a set of finite time intervals, the results for each new step being calculated from

those of the previous step, or from the prescribed initial conditions, by means of the finite-difference approximations to the differential equations.

Such a finite-difference approach, described in detail elsewhere,^{1,2} immediately raises questions concerning accuracy, for which two distinct aspects can be recognized. First there is the question of representing the true physical processes with realistic differential equations and interaction functions for which several comments have already been made. Second, there is the question of the errors introduced by the finite-difference approximations.

The numerical errors are of several different kinds. One arises from coarseness of resolution, and can be mitigated by the use of a mesh scale that is fine compared with the spatial scale for appreciable changes in the field variables, and by time-step intervals that are small compared with the time scale for appreciable local changes. Another is numerical instability in which the calculated results oscillate around the desired solution with increasing amplitude, or otherwise drift away from the desired results.

Numerical instability can sometimes be cured by means of an implicit formulation of the finite-difference equations or by the introduction of a dissipative mechanism, for example, viscosity. The technique we have been using employs both.

The implicitness is required because of our need for flow analysis at very low Mach numbers and/or with strong coupling between the fields. This crucial feature is emphasized in the original reports of the technique and is not discussed further in the present paper.

The introduction of viscosity as a dissipative procedure must be accomplished with great care since numerical stability often requires magnitudes for the viscosity coefficient that greatly exceed the true values for the materials. Specifically, the viscosity must not be so great as to damp excessively the longer wavelength perturbations described in the previous section. For numerical stability, however, the kinematic viscosity, ν , must usually exceed some constant fraction of the product of fluid speed u_0 and mesh-cell size, Δx . Roughly, when the time step per cycle is appropriately chosen, we may estimate for the required viscosity

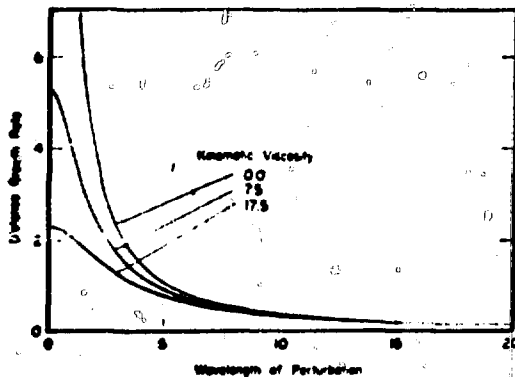


Fig. 1. Instability Growth Rate as a Function of Perturbation Wavelength for Various Kinematic Viscosity Coefficients.

$$u_0 \delta x.$$

Thus, the smaller the cell size, the less viscosity is required. At the same time, Fig. 1 shows that the smaller the viscosity, the smaller is the perturbation wavelength that is essentially unaltered. Thus the two considerations are compatible. For a given physical scale to be resolved, the mesh scale, δx , can be reduced, at least in principle, to the extent that the contortion is resolved, and the viscosity required for numerical stability will have negligible effect on the scale of the contortion.

In practice, this necessary fineness of mesh scale can, indeed, be realized with present computers for many, but not all, problems of interest. The next section describes and illustrates several examples.

VI. NUMERICAL EXAMPLES

In order to demonstrate that long-wavelength instability can be accurately calculated, despite the mitigation of very short-wavelength instability by means of numerical dissipation, we consider the configuration of a fluidized dust bed in which physical instability is well known to occur. Figure 2 illustrates the physical slugging flow for such a dust bed. The calculation commenced from a slightly perturbed equilibrium and developed the oscillatory behavior in a spontaneous and natural fashion. Void fraction as a function of height from the floor of the bed shows a progression of propagating waves with exponentially growing amplitude (in excellent agreement with linearized stability-analysis pre-

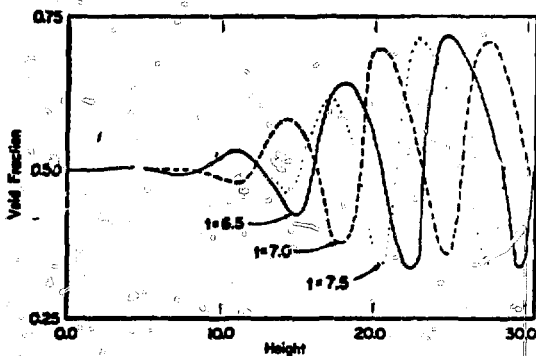


Fig. 2. Void Fraction vs Height from the floor of a Function of Perturbation Wavelength for Various Kinematic Viscosity Coefficients.

dictions) in the lower regions, and an amplitude that is bounded by nonlinear effects in the upper regions. This example demonstrates that physical instabilities can indeed be accurately calculated with neither the disastrous manifestations of short-wavelength instability nor excess smoothing for the dynamics of interest.

Our second example is designed to examine a possible, but highly improbable, scenario of an extremely simplified hypothetical liquid metal fast breeder reactor (LMFBR) disassembly accident. A typical configuration of the core-reflector-plenum region in cylindrical coordinates is diagrammed in Fig. 3. The void contains sodium vapor while the remaining volume is filled uniformly with uranium-dioxide and steel droplets in the core and steel droplets everywhere else. Due to nondissipating power increases in the core region, high vapor pressure can develop,

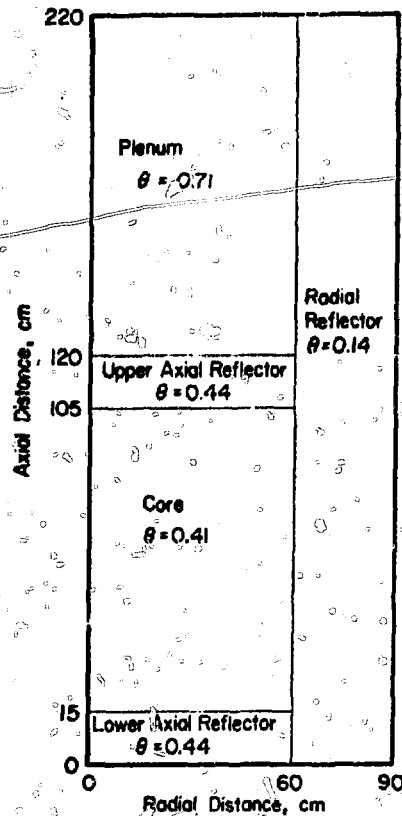


Fig. 3. A Typical LMFBR Core-Reflector-Plenum Configuration. θ denotes the Void Fraction.

resulting in a pressure-driven expansion. The bottom and right-hand boundaries are considered rigid, while material is allowed to enter and exit through the top. A composite of the various fields and their time evolution is presented in Fig. 4. The marker-particle configuration depicts the distribution and density of the various materials throughout the computational mesh. Fuel and steel droplets are represented respectively by the square and plus signs, while sodium vapor is represented by the dots. The velocity fields are normalized to the maximum velocity on the mesh for that particular field.

The calculation progresses with an intense shock developing in front of the sodium vapor expanding out of the pressurized core region. Because of the tight coupling between the vapor and droplet fields, the droplet motion is initially almost coincident with the vapor expansion. The shock deforms and compresses the reflector regions before first impacting the lower boundary and then the right-hand boundary. This results in droplets piling up against these boundaries and developing totally incompressible regions shown by the low or ≈ 0.0 contour line in the void fraction field. The shock reflects off the boundaries, and the sodium vapor streams towards low pressure regions dragging droplets along. In the final stages of the calculation, material is shown to be rapidly exiting the top boundary, and the central region becomes highly voided. Although this example represents an idealized hypothetical LMFBR disassembly accident, it clearly demonstrates the capability of calculating interpenetrating materials in two-phase flow problems.

VII. CONCLUSIONS

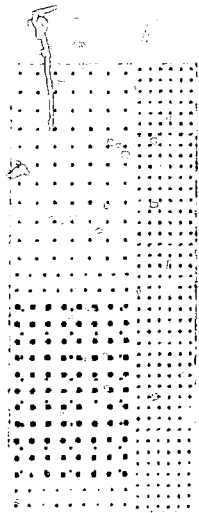
Because most two-phase flow problems are so naturally complicated, high-speed digital computers are being employed to solve the coupled nonlinear partial differential equations that describe the dynamics of such a complex physical system. The formulation of these equations, as reported in the original work, is shown to be correct by a derivation from a statistical viewpoint, which is based on the moments of a Liouville equation. These differential field equations governing the motion of two-phase interactions are "well posed" as illustrated by a fluidized dust bed calculation. In this example we see that the dynamics of resolvable flow contortions can be successfully calculated without requiring excessive dissipation or smoothing, and at the same time avoiding fine scale instabilities that otherwise would destroy the validity of the results.

REFERENCES

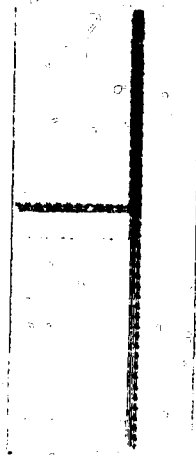
1. F. H. Harlow and A. A. Amsden, "Numerical Calculation of Multiphase Fluid Flow," J. Comp. Phys. 17, 19 (1975).
2. A. A. Amsden and F. H. Harlow, "KACHINA: An Eulerian Computer Program for Multifield Fluid Flows," Los Alamos Scientific Laboratory report LA-5680 (1974).
3. Peter Lax, personal communication.

Fig. 4. Example of a pressure driven disassembly

Time = 0.0 sec

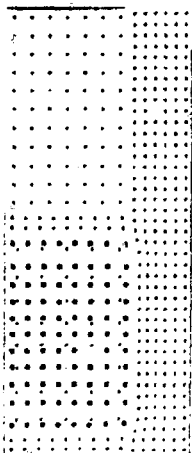


(a) Marker-Particle Configuration

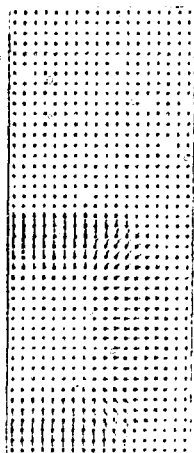


(d) Void fraction

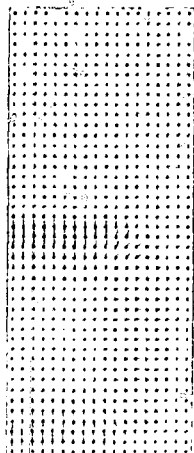
Time = 10^{-3} sec



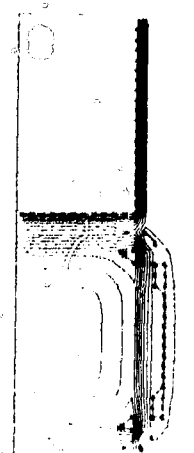
(a) Marker-Particle Configuration



(b) Vapor velocity Field

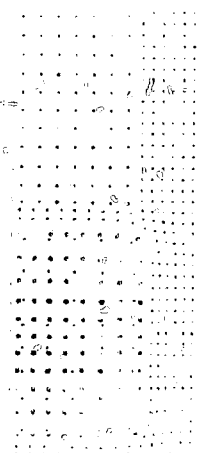


(c) Droplet velocity Field

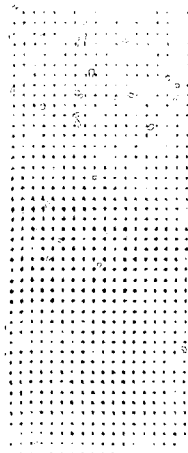


(d) Void fraction

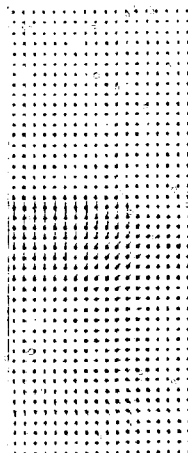
Time = 2×10^{-3} sec



(a) Marker-Particle Configuration



(b) Vapor velocity Field

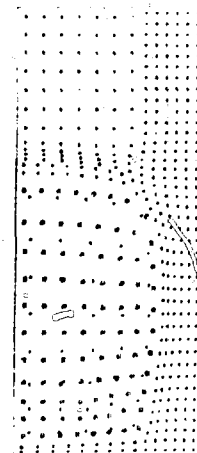


(c) Droplet velocity Field

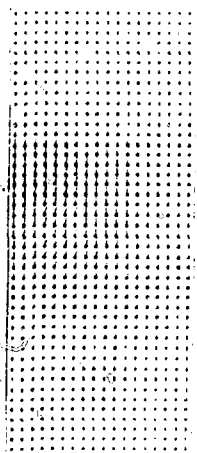


(d) Void fraction

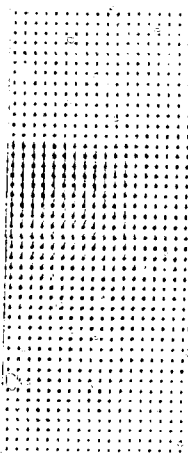
Time = 5×10^{-3} sec



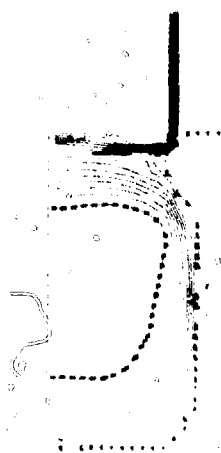
(a) Marker-Particle Configuration



(b) Vapor velocity Field

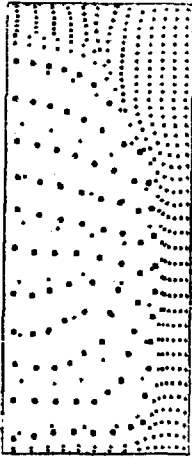


(c) Droplet velocity Field

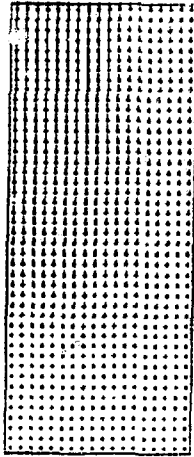


(d) Void fraction

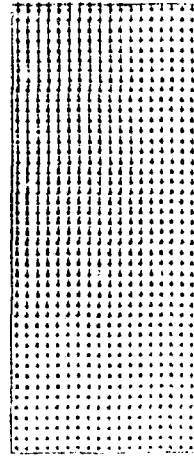
Time = 15×10^{-3} sec



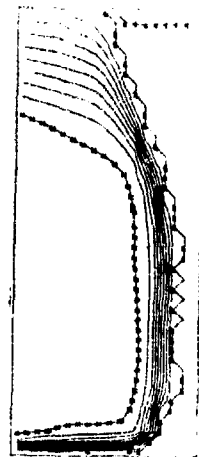
(a) Marker-Particle Configuration



(b) Vapor velocity Field

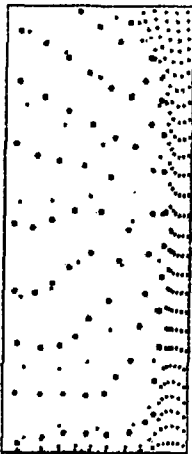


(c) Droplet velocity Field

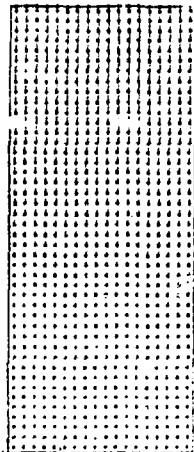


(d) Void fraction

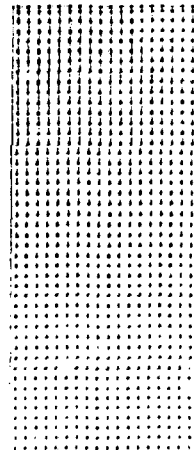
Time = 30×10^{-3} sec



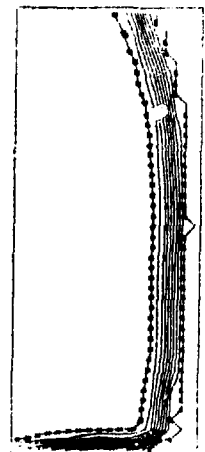
(a) Marker-Particle Configuration



(b) Vapor velocity Field



(c) Droplet velocity Field



(d) Void fraction